EUROPEAN JOURNAL OF MATERIALS SCIENCE AND ENGINEERING
Volume 8, Issue 4, 2023: 226-239 | www.ejmse.ro | ISSN: 2537-4338

EJMSE

DOI: 10.36868/ejmse.2023.08.04.226

EFFECT OF pH ON OPTICAL PROPERTIES OF NANOSTRUCTURED Cu-DOPED ZnS THIN FILMS FOR PHOTOVOLTAIC APPLICATIONS

Mohammad SHAHJAHAN[1*], Rafiul KABIR[1], Mohammad Sajjad HOSSAIN[2], Mohammad Asadul HAQUE[1], Deba Prasad PAUL[1]

[1]Department of Physics, University of Chittagong, Chittagong-4331, Bangladesh
[2]Industrial Physics Division, BCSIR Laboratories Dhaka, Bangladesh Council of Scientific & Industrial Research (BCSIR), Dhaka -1205, Bangladesh

Abstract

Using the simple Chemical Bath Deposition (CBD) method, Cu-doped thin films of zinc sulfide (ZnS) were deposited on glass substrates in a concentration range of 0.05-0.1% Cu. These films were made to be used as a buffer or window layer in solar cells. Different deposition conditions were investigated to find the optimal growth conditions; after that, the conditions were deployed to deposit the required films. XRD graphs confirmed a hexagonal structure, and SEM images indicated that the incorporation of Cu stabilises small grain growth in the films. The appearance of the sample surface was dense, with an ordered granular shape, and free of any cracks. The optical and surface properties of the prepared films have been analysed using state-of-the-art instruments. The effect of pH on such properties has also been investigated. The transmittances of the films were about 20–85%, and the incident wavelength range was 300–1100 nm. The transmission line shows a sharply increasing tendency. After that, it increases slowly and goes to a stable state above 400 nm. A film of pH 10.0 showed a high transmission coefficient (85%). Also, the absorbance of the ZnS thin films rapidly decreases up to 360 nm. After that, it decreases slowly and becomes stable above 400 nm. The band gap is in the range of 3.58–3.62 eV, which indicates that it absorbed the UV portion of the electromagnetic wave and could be used as the UV filter.

Keywords: *Solar Cell, Photovoltaics, Zinc sulfide, Metal sulfide, Chemical bath, Optical properties.*

Introduction

Nanoscience and nanotechnology are the study and usage of incredibly small things, and they can be used in science to describe a new perspective on and method of study. A bridge between science and technology has been built. Low-dimensional materials and structures have exceptional qualities that make it possible for them to be instrumental in the rapid advancement of science. Because it bridges the gap between bulk and atoms or molecules [1][2][3] the study of materials at the nanoscale has attracted a lot of attention. This interest is spurred by the shrinking manufacturing process for optoelectronic and electrical devices.

Semiconductors are materials that have conductivity between a conductor and an insulator. They are available in nature in both the form of elements and compounds. Silicon and Germanium are known as the most common and useful elements in semiconductors. Also, some other compounds as semiconductors are available, such as GaP, PbS, ZnO, ZnS, etc. Among the three types of materials, semiconductors are very important as they have the property of varying conditions like temperature and impurities [4] that can frequently alter their conductivity. It has the property to cover the transition from the bulk to molecular scale, which gives the possibility

*Corresponding author: shahjahan@cu.ac.bd

to draw a perfect model to observe, study, and characterised the size-dependent and morphological, structural, and physical properties that arise from the charge carrier motion.

Metal sulfides like ZnS or ZnSe are important semiconductor materials with a wide direct band gap of 3.6–2.6 eV within the UV range [5]. It has some general properties, like being cubic in structure and having the form of a powder or crystal with a white to yellow colour. It shows the molecular mass is 97.474 g mol^{-1} and the density is 4.090gcm^{-3}. The cubic form showed a band gap of 3.54 eV [6] at 300 K. On the other hand, the hexagonal form showed a band gap of 3.91 eV [7].

Solar cells have become a popular energy technology that provides power by absorbing solar energy from the sun. Thin film deposition is a sensitive technique where a layer of a very small thickness of the expected material is deposited on the substrate to get the absorption, which can be used in electronics, semiconductor devices, and electrical sensors [8]. Sometimes a second or third layer is deposited on the first layer to increase the efficiency of the device, popularly known as second-generation solar cell technology [9]. Different types of suitable substrates may be used for the layer deposition of one or more thin layers using different photovoltaic materials [7] such as ZnS, ZnO, CuS, CuO, ZnSe, CdTe, or CIGS [10]. Deposition, by controlling the thickness of the film, can be used as an absorber layer or buffer layer in a solar cell [11].

Structures of materials with low dimensions showed outstanding properties and played a very important role in the field of science. Nanostructures with one dimension have become the centre of attraction in the natural sciences. The experiment at the nanoscale has a chance to fill the research gap in optoelectronics and electronic device fabrication. A thin film is just a layer of the expected research material with a thickness in the nanometer to micrometre range. It is used in semiconductor devices and optoelectronic coatings [12]. The process of creating a thin-film photovoltaic cell (TFPV), also referred to as a second-generation solar cell, involves depositing one or more thin layers of photovoltaic materials on various substrates like glass, plastic, or metal [13]. The deposition technology is used in several methods, such as cadmium telluride (CdTe), copper indium gallium diselenide (CIGS), and thin-film silicon (a-Si, TF-Si). Generally, thin film-based solar cells such as $CuGaIn(S, Se)_2$ absorbers or CdS (Cadmium Sulfide) are used as a buffer layer, which is required to get high efficiency for energy conversion [14].

But toxicity is the main issue that arises with production and the use of hazards within the CdS layer. To minimise the problem, scientists are trying to develop cadmium-free buffer layers. In this research, we are trying not to use a toxic material, which leads us to investigate ZnS as a buffer layer in $ZnO/ZnS/CuInS_2$ devices. Metal sulfide like ZnS, which has a large band gap in comparison with CdS, allows excess photons to be transmitted into the junction, which gives the blue region activation of the spectrum line of the designed solar cells.

Scientist Vincenzo Cacariolo placed barium sulfide as a luminous host in the year 1603 [15]. Following that, other scientists created more luminous hosts. Other metal sulfides such as calcium sulfide (1700), strontium sulfide (1817), and zinc sulfide (ZnS) (1866) were also successfully deposited by three other scientists [16]. Destriau developed responsive ZnS in 1936 [17]. Following that, it has been extensively employed as EL materials and as research instruments. ZnS can be utilized as a blue color responder, but other transition metals must be substituted if you want longer wavelength responses.[18]. By reducing size while enhancing other qualities, scientists can experiment with metal sulfides such (ZnS), metal oxide (ZnO), or Cadmium Sulfide (CdS) [18]. Scientists find it more difficult to do research with this material than ZnO since it has several unique characteristics like a broad bandgap (3.7). Additionally, CdS is now the most popular semiconductor for use as a buffer layer in solar cell devices, however scientists have rejected it due to its toxicity and narrow energy bandgap [19].

In order to study the aforementioned zinc sulfide (ZnS) deposition on glass substrates, Nasr et al. changed the pH range of the solution from 10 to 11.5 [20]. They discovered that the effects of an elevated pH value enhance visible-range transmission. And a high 70% transmission

coefficient was recorded. Additionally, at a pH of 11.5 the direct band gap energy was 3.67 eV, which was slightly high.

A better CBD technique, in which substrates were heated before being doped with the reaction solution, was reported by H. Lekiket et al. [21]. They claimed that the surface was homogeneous and compact, and that the films' Zn/S composition ratio was 52:48. After applying the correct annealing, Roy et al. demonstrated that the ZnS films formed excellent crystals with pure-wurtzite structures [22]. The produced films in this instance displayed excellent optical characteristics with high transmittance and a high bandgap value of 3.69 eV. According to the report, films have a high optical transmission of 80–100% when the annealing temperature is raised to 500°C, which is very beneficial for solar cells.

It has a large application in photovoltaic cells [23], [24], electroluminescent devices [25], blue light-emitting diodes [26], and anti-reflection coatings as well [27], ZnS, which is non-toxic and harmless, is employed for these thin films, as CdS is poisonous and dangerous for human health and the environment [28]. Compared to CdS, ZnS has a broader band gap, which facilitates the transfer of energetic photons through the junction [29]. ZnS thin films have been prepared using a variety of film preparation techniques, including thermal evaporation, chemical bath deposition [30], (CBD), chemical vapour deposition [31], (CVD), molecular beam epitaxy [32], metal-organic vapour phase epitaxy [33], spray pyrolysis [34], and sol-gel method [35].

Of these, the CBD approach seems appealing for its cheapness. It does not need any complicated equipment for vacuum or high-temperature production. This procedure is often carried out when temperatures are below 100 degrees and at atmospheric pressure [36]. Besides, it has some downsides as well, like in large-scale manufacturing, where CBD leads to huge liquid waste. ZnS, used in this process, precipitates quickly and has a poor solubility product (10–24.7), which causes the rough surface in the thin film. [37].

Among these many deposition processes, we are trying to find the easiest and most cost-effective economic deposition process, which is chemical bath deposition. It is the technique that is currently getting attention, as it is simple and time-saving, needs a small amount of material, and the wastage is too small. This technique needs a simple instrument and can be useful in large-area deposition with a low or room temperature. Thin films formed using metal sulfide or metal selenide have been used in various devices. The major applications of this type of thin film cover a wide area of interest, such as coating as anti-reflection for the solar cell [38], buffer layer fitted with the environment in replacing the CdS layer in CIS-based thin film solar cells [39], Electroluminescent and optoelectronic devices to serve the purpose of wide bandgap [40], Photosynthetic coating [41], blue light-emitting laser diodes [42], and alpha-particle detector.

Literal analysis offers us the impression that we can take a chance and use a layer of ZnS thin films instead of a layer of CdS thin films because of its higher bandgap, which would result in higher absorption of shorter wavelengths. Finally, we can state that ZnS would be a good replacement for the CdS layer because it can be used to create environmentally benign solar devices [43].

In this research, we have made several samples of ZnS thin films deposited on different types of glass substrates. Glass substrates with or without Cu doping are used to get absorber layers for the new type of solar cell device. The deposited film is checked for its different physical and optical properties, like film thickness, transmittance, and structural and surface morphology. With a straight and wideband gap (E_g = 3.6 eV), ZnS is one of the most significant semiconductors in the II-VI group.

Materials and Method

On glass substrates, the Chemical Bath Deposition (CBD) method produced the ZnS thin films. All experiments were carried out initially at room temperature without further temperature control. 50 ml of 1M $Zn(CH_3COO)_2$, 10 ml of 3.75M triethanolamine (TEA), 50 ml ammonia (NH_3), 16 ml of 0.66M trisodium citrate ($C_6H_5Na_3O_7$) and 50 ml of 1M thiourea were taken

primarily to start the deposition. Firstly, zinc acetate and trisodium citrate solutions were prepared and mixed with a stirrer for 30 minutes. A clear solution is seen in the beaker. After that, ammonia and thiourea solutions were slowly added to confirm the buffer state of the solution. Again, TEA was added slowly to the solution with rigorous stirring for up to 30 minutes until a stable solution was formed. The pH of the solution is adjusted and kept at 10 to 11.5 by adding Ammonia. The substrates were dipped in the solution for 3 hours and kept in the microwave oven at a temperature of 90 °C for 18 to 48 hours. After deposition, the prepared thin films were washed using enough distilled water and then kept in the open air to dry. Before the deposition, the glass slides were cleaned properly using an ultrasonic cleaner and distilled water. The glass slides were placed vertically in the reaction chamber. After that, 5 ml of 0.01M $cucl_2$ and 5 ml of 0.02M $cucl_2$ were used as doping elements. All samples were prepared by varying the pH and concentration of the ammonia solution. After that, the deposited ZnS samples were then annealed at 90 °C for different times (such as 18 h, 24 h, 40 h, and 48 h) in an argon environment to investigate the annealing effect. The respective instruments then took optical, structural, and morphological measurements.

Results and Discussion

Optical characterization of ZnS thin films

The absorbance and transmittance of the deposited film were determined by the UV-visible spectrophotometer within the wavelength range of 200–1100 nm. Both absorbance and transmittance were checked in two ways. First by keeping the pH constant and then by changing it. Absorbance and transmittance characteristics are shown in the following figures:

Effect of concentration variation on absorbance at constant pH

Fig. 1 (a, b, c, and d) shows the absorption spectra of different doped and undoped samples. Every sample group was checked, keeping the pH constant for that group but different for other groups, and the pH was 10, 10.5, 11, and 11.5 respectively. Figures indicate that, undoped sample without Cu doping, where pH was 10.0, showed the highest absorbance pick at the low-frequency range, but the second sample group (0.1MCu) showed it at the high-frequency range. The absorbance pattern is almost similar for all sample groups and rapidly decreases near 320 nm. In the region higher than 320 nm, its decreasing trend goes slowly, and it gets a stable state above 360 nm, except for the second sample group. For the second sample group indicated in Fig. 1b, 0.1MCu doped sample showed an absorption decrease up to 340 nm. After that, it stays stable between 380 and 400 nm. It showed higher absorption in the stable states.

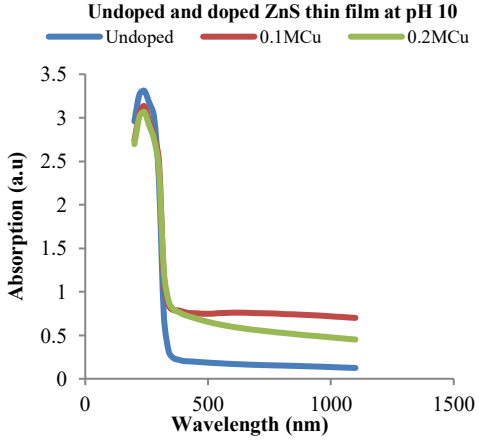

a)

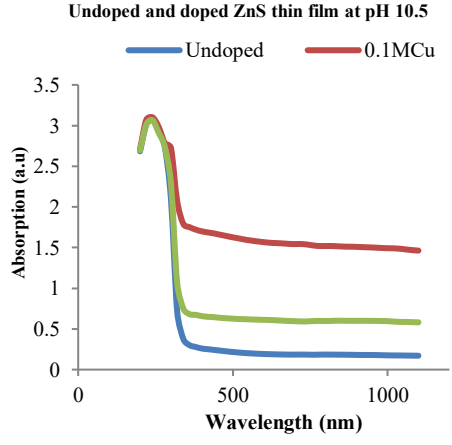

b)

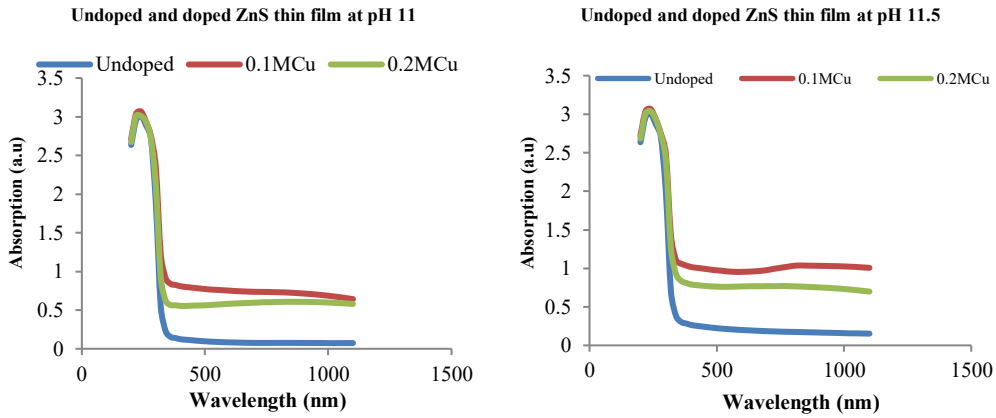

c) d)

Fig. 1. UV-Vis absorption spectra of ZnS thinfilms prepared at four dofferent pH: a) 10.0; b) 10.5; c) 11.0; d) 11.5.

All figures indicate that increasing pH decreases absorption.

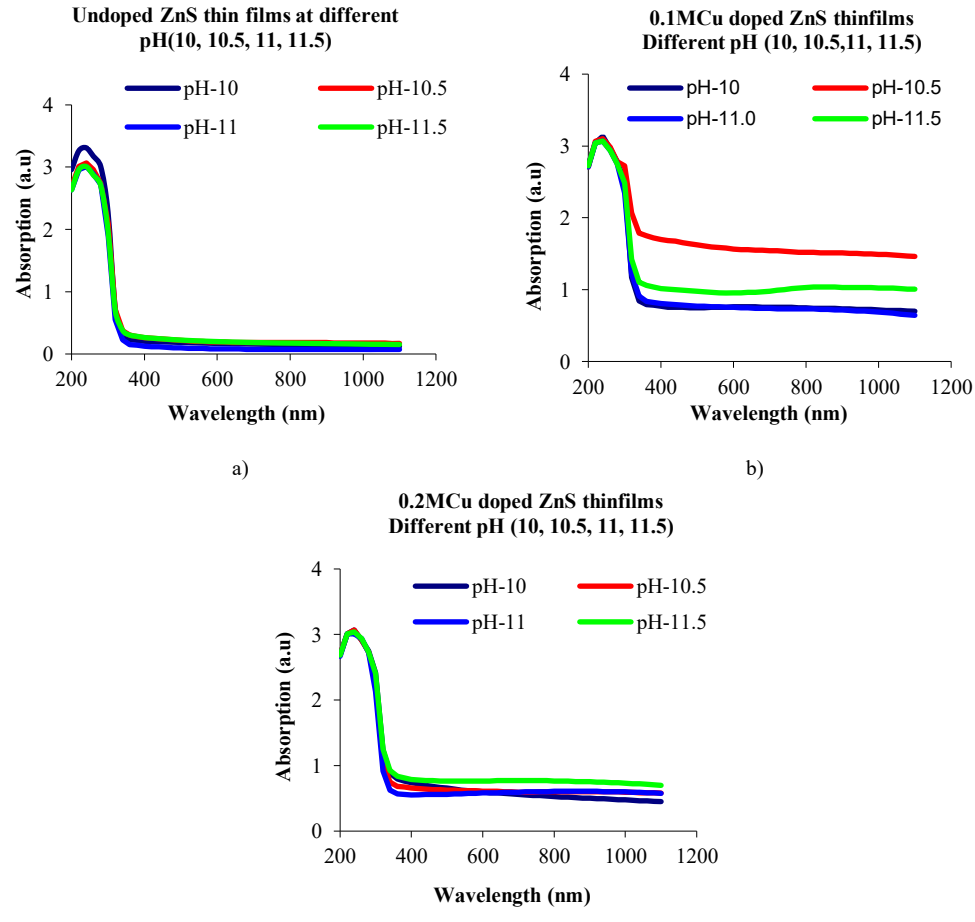

a) b)

c)

Fig. 2. UV-Vis absorption spectra of doped and undoped ZnS thinfilms: a) without Cu; b) 0.1M Cu; c) 0.2M Cu

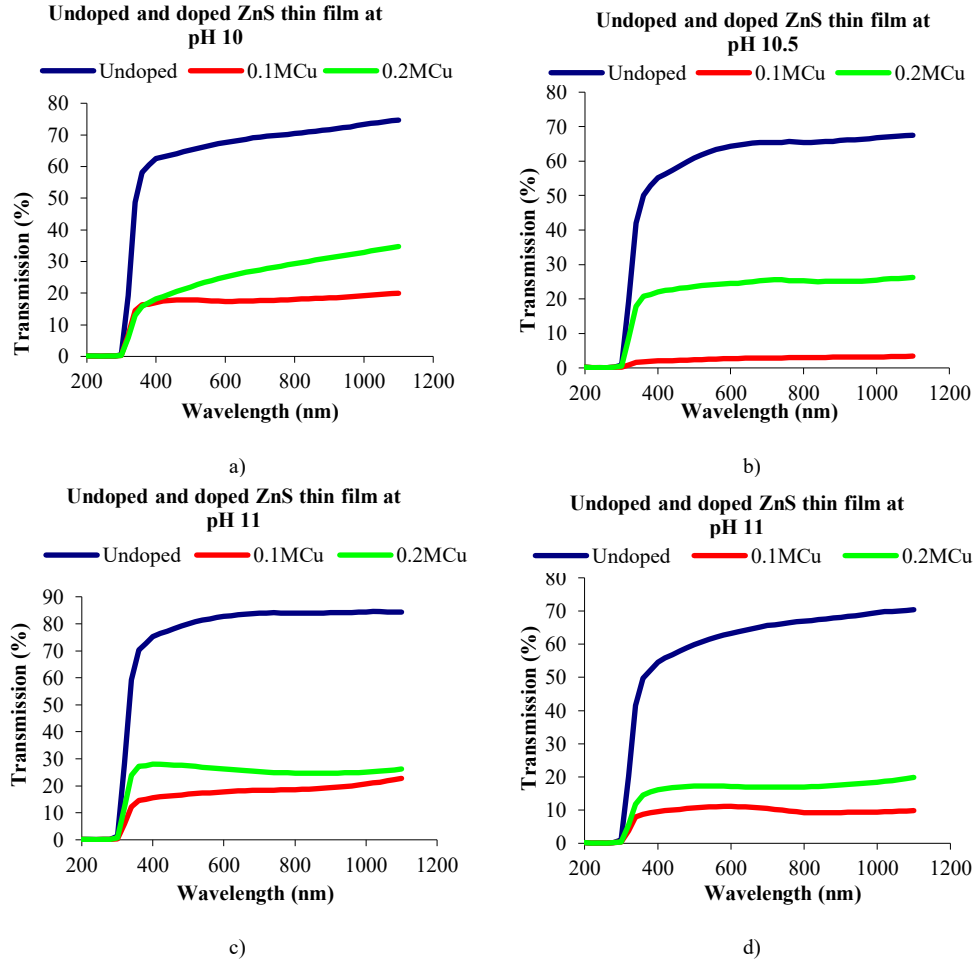

Fig. 3. UV-Vis transmission spectra of ZnS thinfilms prepared at four dofferent pH:
a) 10.0; b) 10.5; c) 11.0; d) 11.5

Band Gap Measurement

ZnS thin films deposited at optimised conditions on glass substrates were characterised by the optical absorption process. The band gap (E_g) for ZnS films was calculated by plotting $(\alpha h\nu)^2$ versus the eneof they of photon ($h\nu$). Here, the corresponding wavelength is (λ), α is the coefficient of absorption. α can be measured from the data of transmittance or absorbance. In this study, we used absorbance data and Lambert's law for measuring the α. [45]. Here:

$$2.303A = \alpha d \tag{1}$$

$$\alpha = \frac{A_o(h\nu - E_g)^n}{h\nu}; \quad n = 0.5 \text{ or } 2 \tag{2}$$

Where $h\nu$ is the photon energy of photons, E_g is the energy band gap, A_o is a constant, A is the optical absorbance, and d is the film thickness estimated by the gravimetric method. The value of n is equal to 0.5 for direct band gap material and 2 for indirect band gap material [46]. Since ZnS is a direct band gap material. So, we used the value of n to equal 0.5.

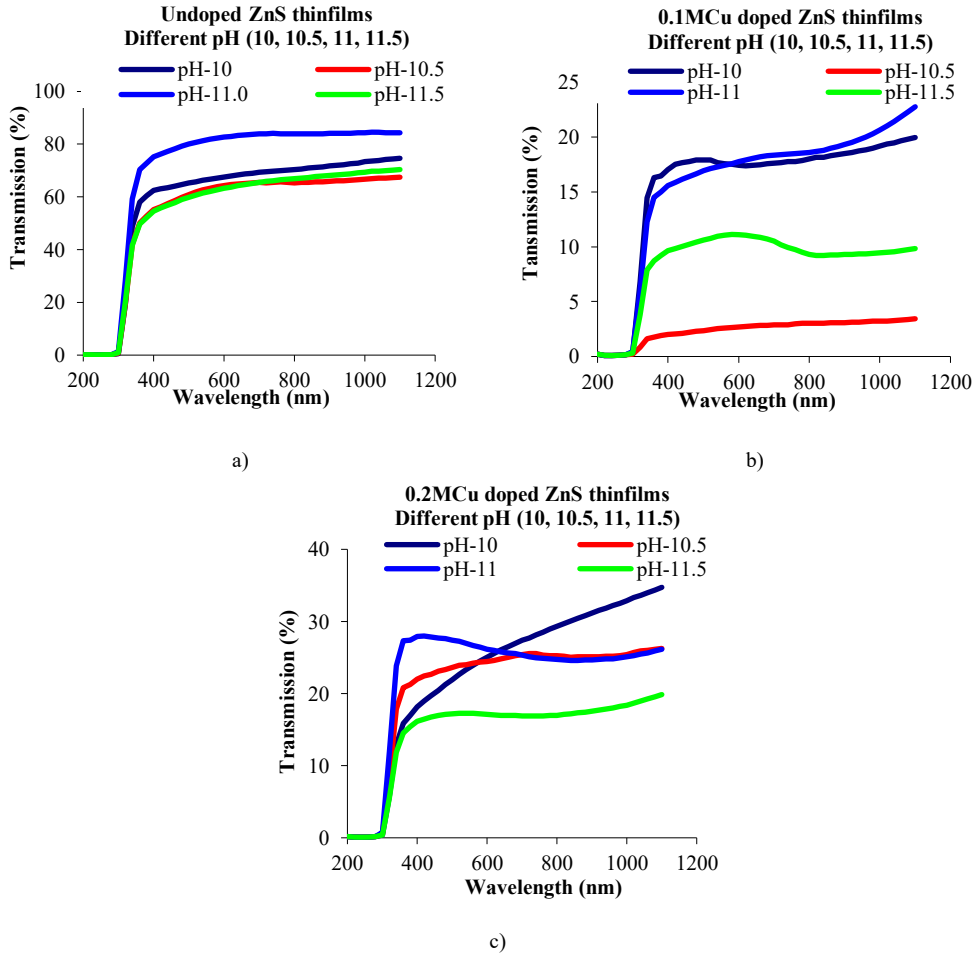

Fig. 4. UV-Vis transmission spectra of doped and undoped ZnS thinfilms: a) without Cu; b) 0.1M Cu; c) 0.2M Cu

$$\alpha = \frac{A_o(h\nu - E_g)^{0.5}}{h\nu} \tag{3}$$

$$(\alpha h\nu)^2 = A_o^2(h\nu - E_g) \tag{4}$$

Extrapolating the straight-line portion of the curve in the energy axis gives the values of band gap energy (E_g). The effect of pH on the band gap of the thin films is shown in Fig. 5, and the measured optical band gap and its related pH are shown in Table 1. As shown in Fig. 5, the energy bandgap values lie within the range of 3.58 to 3.62.

At pH = 10 and pH = 11, band gap energy (E_g) equals to 3.62 eV, which is very close to bulk ZnS (3.65 eV) band gap [47].

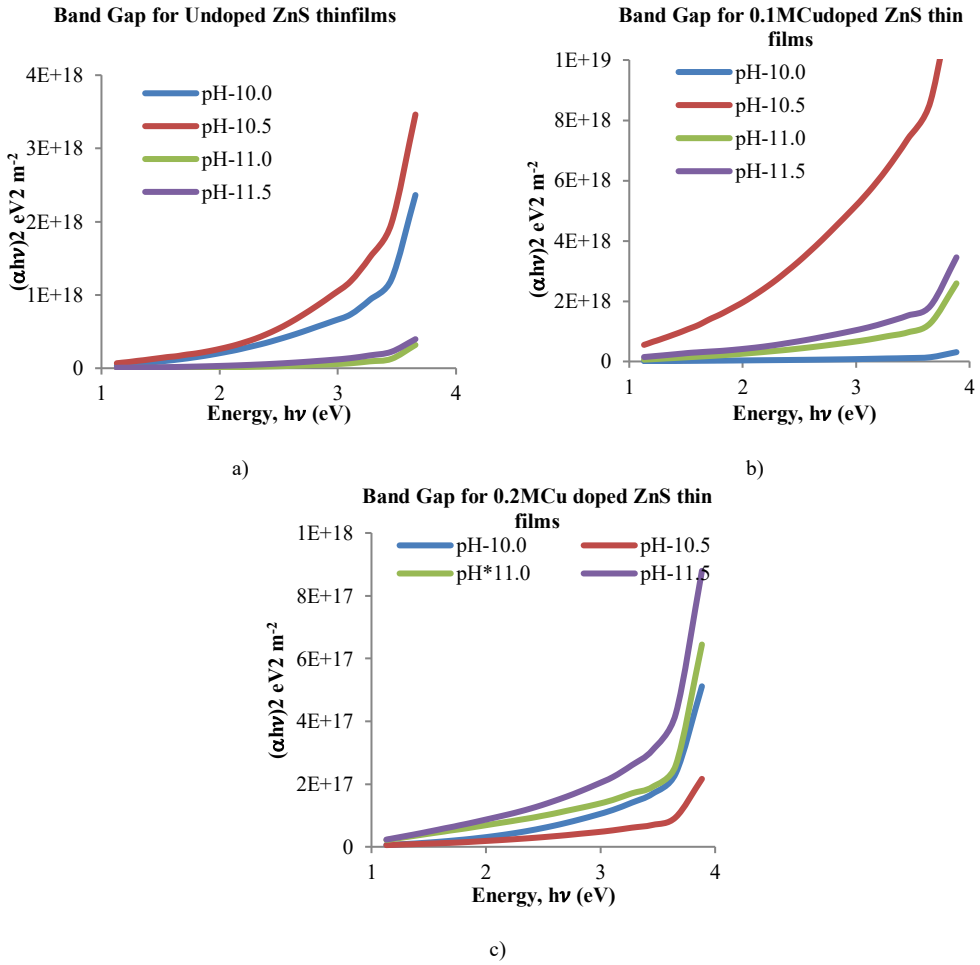

Fig. 5. Plot of (αhν)2 versus photon energy (hν) for ZnS thin films: a) withoup Cu; b) 0.1MCu; c) 0.2MCu

Table 1. The optical band gap for all samples with different pH

Without Cu		0.1M Cu		0.2M Cu	
pH value	**Optical band gap, E_g (eV)**	**pH value**	**Optical band gap (eV)**	**pH Value**	**Optical band gap (eV)**
pH 10.0	3.62	pH 10.0	3.47	pH 10.0	3.48
pH 10.5	3.60	pH 10.5	3.24	pH 10.5	3.50
pH 11.0	3.62	pH 11.0	3.46	pH 11.0	3.51
pH 11.5	3.58	pH 11.5	3.40	pH 11.5	3.47

X-ray diffraction measurements

Structural Properties

The X-ray diffraction patterns for the investigated films have been shown in Fig. 6. Powder diffraction by an X-ray powder diffractometer was used to find the crystalline phases using (Cu–Kα) =1.5406 AA with a step size of 0.02, 2$\theta\circ$ at room temperature. The structural parameters of all the samples, such as the lattice parameters, are calculated from the XRD data. All the sharp peaks are in the same position as stated in the literature [38]. which confirmed the sample formation was accurate and has a single phase only. The lattice constant is calculated by using the known eq. (5).

$$a = d_{hkl}\sqrt{h^2 + k^2 + l^2} \tag{5}$$

where the Miller indices are h, k, l and interplanar spacing is d_h.

It is observed that the highest intensity peak is at the 38° position. The calculation gives the peak as (311) plane, which tells us the prepared sample has the characteristics of ZnS. The average size of the crystal bulk sample (D_p) is calculated using the Scherrer eq. (6) [48].

$$D_p = \frac{0.94l}{\beta cos\theta} \tag{6}$$

Where the line broadening in radians is β, the Bragg angle θ and the X-ray wavelength λ. Also, each of these peak patterns (111), (220), and (311), is observed, telling us the structure of the cubic zinc blend structure (cubic, β-ZnS). It is found that changes in temperature and the bath can't have any effect on the crystal structure of films. The typical broadening size from the spectra of diffraction peaks shows that the size of ZnS is very small. The values of particle size obtained from XRD for different films are measured and tabulated.

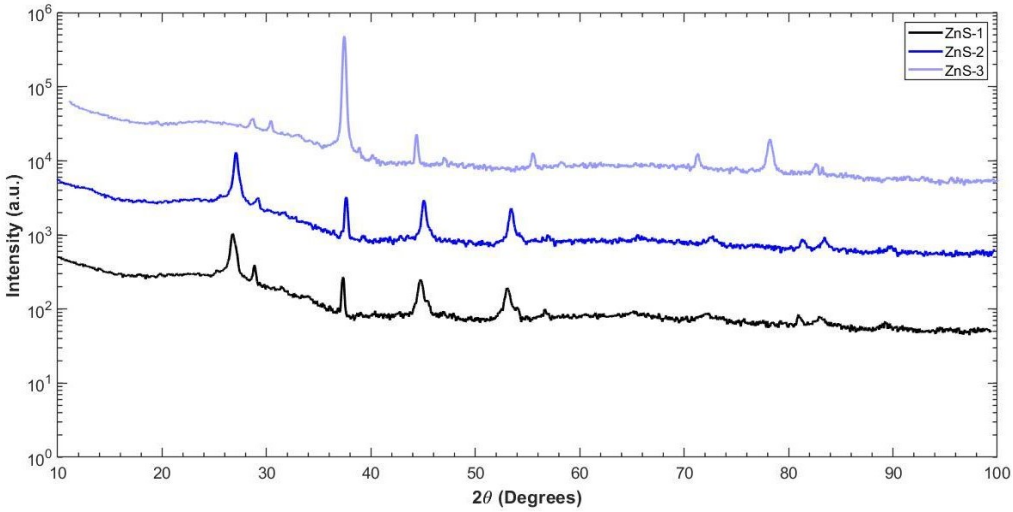

Fig. 6. XRD patterns of ZnS thin films ZnS-1 (without Cu), ZnS-2 (0.1M Cu) and ZnS-3 (0.2M CU) doping

Morphological characterizations of ZnS thin films

Scanning Electron Microscopy (SEM) Measurements

The images of microstructure for the ZnS thin films were observed by SEM to get microscopic information on the surface structure and roughness**.** Images were taken at different magnifications, as shown in Fig. 7, for all samples. Images showed that the sample has homogeneity and is composed of agglomeration and isolation. The grain sizes vary from 26 to 34 nm. Images showed that the substrate didn't have any major cracks or pinholes, which means it was well covered with the deposited material. Also, it is observed that small particles are aggregated into secondary particles because of their small dimensions and high surface energy.

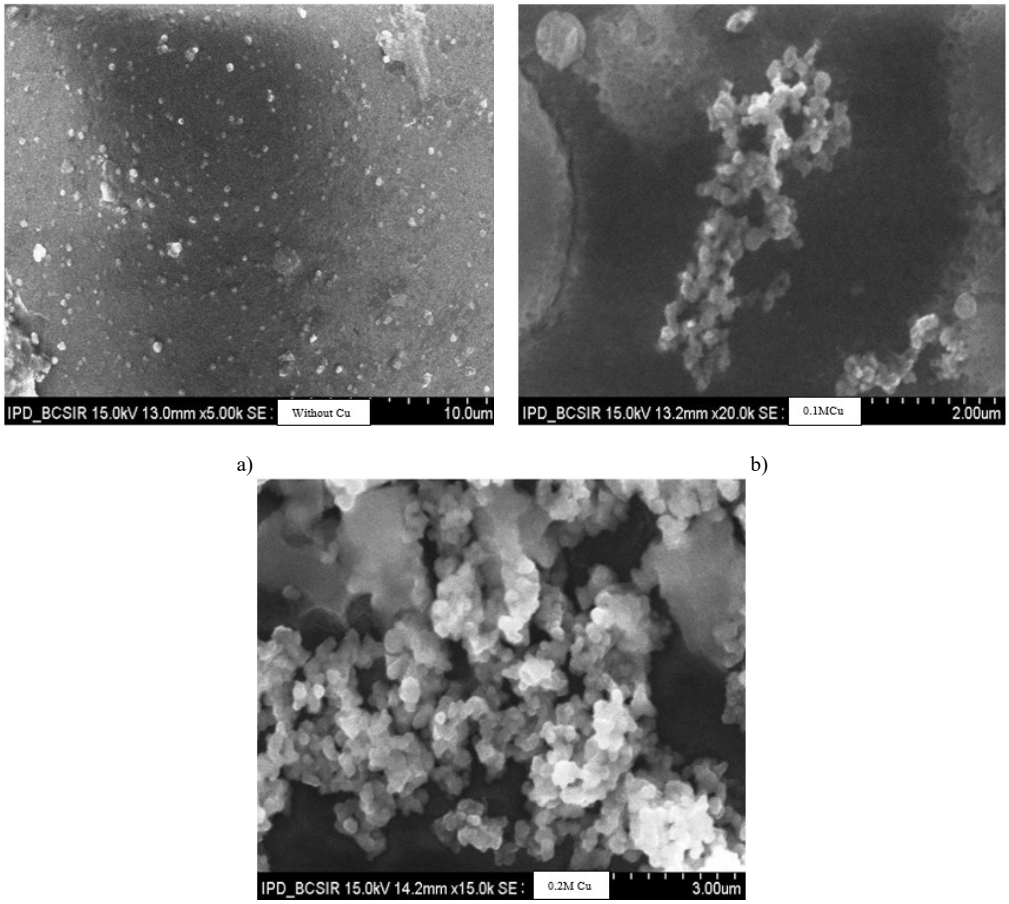

a) b)

c)

Fig. 7. SEM image of the surface of ZnS thin films top layers

A slight increase in the grain size follows the increase in the effect of pH but does not improve the surface roughness.

Conclusions

The synthesis and deposition of the ZnS thin films using co-precipitation and dip coating methods while maintaining proper deposition conditions are reported. The deposition conditions have been optimized to get a better-quality thin layer. The grown layers of ZnS have been characterized by UV-visible spectrophotometers for optical transmission and reflection properties, SEM for surface morphology, and X-ray diffraction technology for structural properties. The effects of pH and deposition time have also been investigated. These investigations showed that the pH has a direct effect on the growth conditions and plays a vital role in the formation of depositions and the structure of the films. From the observation, we got the best crystalline character where pH was 10. The decrease in the pH value from 11.5 to 10 is related to the increase in the transmittance property. Optical measurement showed that the transmittance was about 20–85%. Transmittance increased sharply to 300–360 nm, and after that, it increased slowly and became stable above 400 nm. The optical transmission coefficient showed

an increasing tendency with the lowering of pH, and at pH 10.0, we got a high transmission coefficient nearing 85%.

Also, the absorbance of the Zn thin films decreases sharply up to 360 nm, decreases slowly up to 400 nm, and becomes stable after 400 nm. The UV-Visible spectra revealed that there is a chance to use the film as a UV filter and window layer of the solar cell. The UV data shows that the band gap of the film is in the range of 3.58–3.62 eV. XRD spectra supported the formation of ZnS thin films and the crystal information, including size. From XRD spectra, the particle size is calculated at about 30–40 nm using the Debye–Scherrer formula. The morphology of films has also been studied using SEM images and analyzed. SEM analysis indicates that the ZnS thin films have the expected homogeneity and uniform morphology. Bandgap indicates the absorption range of the electromagnetic spectrum, which is near UV light. So, it is concluded that the prepared films have the potential to be an absorber or window layer of the solar cell. The band gap of ZnS is wider than that of CdS (which is 2.42 eV). Therefore, it can replace CdS in CIGS absorber-based solar cells where CdS is used as a buffer layer. To account for the toxicity of Cd, it can be immediately concluded that ZnS thin film is more suitable for use as a window or buffer layer than CdS.

Acknowledgement

We would like to highly acknowledge to Research and Publication Cell, University of Chittagong, and the Department of Physics, University of Chittagong, and the authority of University of Chittagong for providing us the grant and opportunity and necessary permission to carry out this research work. Thanks are also due to all the employees of the Industrial Physics Division, BCSIR Laboratories, Dhaka. Special thanks to Director, BCSIR Laboratories Dhaka for giving us all the research facilities.

References

[1] A. Raidou *et al.*, *Characterization of ZnO Thin Films Grown by SILAR Method*, **OALib**, **01**, **(03)**, pp. 1–9, 2014, doi: 10.4236/oalib.1100588.

[2] S. Kulkarni, *Innovations in Green Nanoscience and Nanotechnology*. **Boca Raton: CRC Press**, 2022. doi: 10.1201/9781003319153.

[3] J. Andreo *et al.*, *Reticular Nanoscience: Bottom-Up Assembly Nanotechnology*, ***J. Am. Chem. Soc.***, **144**, **(17)**, pp. 7531–7550, May 2022, doi: 10.1021/jacs.1c11507.

[4] V. Parthasaradi, M. Kavitha, A. Sridevi, and J. J. Rubia, *Novel rare-earth Eu and La co-doped ZnO nanoparticles synthesized via co-precipitation method: optical, electrical, and magnetic properties*, **J. Mater. Sci. Mater. Electron.**, **33**, **(34)**, pp. 25805–25819, Dec. 2022, doi: 10.1007/s10854-022-09272-9.

[5] G. Brammertz *et al.*, *Fabrication and characterization of ZnS and ZnSe absorber layers for UV-selective transparent photovoltaics*, **Thin Solid Films**, **767**, p. 139671, Feb. 2023, doi: 10.1016/j.tsf.2023.139671.

[6] M. J. E, M. A. Manthrammel, P. A. Subha, M. Shkir, and S. A. Alfaify, *Microwave-assisted synthesis of praseodymium (Pr)-doped ZnS QDs such as nanoparticles for optoelectronic applications*, **Luminescence**, Sep. 2023, doi: 10.1002/bio.4577.

[7] R. Maity and K. K. Chattopadhyay, *Synthesis and optical characterization of ZnS and ZnS:Mn nanocrystalline thin films by chemical route*, **Nanotechnology**, **15**, **(7)**, pp. 812–816, Jul. 2004, doi: 10.1088/0957-4484/15/7/017.

[8] A. D. Dinsmore, D. S. Hsu, H. F. Gray, S. B. Qadri, Y. Tian, and B. R. Ratna, *Mn-doped ZnS nanoparticles as efficient low-voltage cathodoluminescent phosphors*, **Appl. Phys.**

Lett., **75**, **(6)**, pp. 802–804, Aug. 1999, doi: 10.1063/1.124518.

[9] Y. Wang *et al.*, *Research progress in doped absorber layer of CdTe solar cells*, **Renew. Sustain. Energy Rev.**, **183**, p. 113427, Sep. 2023, doi: 10.1016/j.rser.2023.113427.

[10] J. Tittel *et al.*, *Fluorescence Spectroscopy on Single CdS Nanocrystals*, **J. Phys. Chem. B**, **101**, **(16)**, pp. 3013–3016, Apr. 1997, doi: 10.1021/jp963801q.

[11] S. Mahamuni, K. Borgohain, B. S. Bendre, V. J. Leppert, and S. H. Risbud, *Spectroscopic and structural characterization of electrochemically grown ZnO quantum dots*, **J. Appl. Phys.**, **85**, **(5)**, pp. 2861–2865, Mar. 1999, doi: 10.1063/1.369049.

[12] P. Koralli, S. Fiat Varol, G. Mousdis, D. E. Mouzakis, Z. Merdan, and M. Kompitsas, *Comparative Studies of Undoped/Al-Doped/In-Doped ZnO Transparent Conducting Oxide Thin Films in Optoelectronic Applications*, **Chemosensors**, **10**, **(5)**, p. 162, Apr. 2022, doi: 10.3390/chemosensors10050162.

[13] M. R. Y. Hamid, N. M. Julkapli, M. F. Murshed, M. S. Busnak, M. I. Hilmi, and M. A. M. Adnan, *The effect of MnO concentration on the formation of MnO/ZnO thin films with bifunctional thermal insulation and photocatalytic self-cleaning performance*, **Int. J. Mater. Prod. Technol.**, **65**, **(1)**, p. 80, 2022, doi: 10.1504/IJMPT.2022.124260.

[14] B. M. Sakunde, N. B. Chaure, S. Patole, S. R. Jadkar, and H. M. Pathan, *Numerical Modeling to Improve the Efficiency of Cadmium Sulfide/Copper Indium Sulfide (CdS/CuInS2) Thin Film-based Solar Cells*, **ES Energy Environ**., 2022, doi: 10.30919/esee8c784.

[15] A. Khare, S. Mishra, D. S. Kshatri, and S. Tiwari, *Optical Properties of Rare Earth Doped SrS Phosphor: A Review*, **J. Electron. Mater.**, **46**, **(2)**, pp. 687–708, Feb. 2017, doi: 10.1007/s11664-016-4988-1.

[16] Y. Wu, Y. Shao, and L. G. Jacobsohn, *Luminescence of ZnS:Ag scintillator prepared by the hydrothermal reaction method: Effects of reaction temperature and time, Ag concentration, and co-doping with Al*, **Opt. Mater. (Amst).**, **107**, p. 110015, Sep. 2020, doi: 10.1016/j.optmat.2020.110015.

[17] J. Jaeck *et al.*, *Room-temperature electroluminescence in the mid-infrared (2-3 μm) from bulk chromium-doped ZnSe*, **Opt. Lett.**, **31**, **(23)**, p. 3501, Dec. 2006, doi: 10.1364/OL.31.003501.

[18] X. Fang, Y. Bando, U. K. Gautam, C. Ye, and D. Golberg, *Inorganic semiconductor nanostructures and their field-emission applications*, **J. Mater. Chem.**, **18**, **(5)**, pp. 509–522, 2008, doi: 10.1039/B712874F.

[19] J. Y. Park, R. B. V. Chalapathy, A. C. Lokhande, C. W. Hong, and J. H. Kim, *Fabrication of earth abundant Cu2ZnSnSSe4 (CZTSSe) thin film solar cells with cadmium free zinc sulfide (ZnS) buffer layers*, **J. Alloys Compd.**, **695**, pp. 2652–2660, Feb. 2017, doi: 10.1016/j.jallcom.2016.11.178.

[20] T. Ben Nasr, N. Kamoun, M. Kanzari, and R. Bennaceur, *Effect of pH on the properties of ZnS thin films grown by chemical bath deposition*, **Thin Solid Films**, **500**, **(1–2)**, pp. 4–8, Apr. 2006, doi: 10.1016/j.tsf.2005.11.030.

[21] H. Lekiket and M. S. Aida, *Chemical bath deposition of nanocrystalline ZnS thin films: Influence of pH on the reaction solution*, **Mater. Sci. Semicond. Process.**, **16**, **(6)**, pp. 1753–1758, Dec. 2013, doi: 10.1016/j.mssp.2013.06.028.

[22] P. Roy, J. R. Ota, and S. K. Srivastava, *Crystalline ZnS thin films by chemical bath deposition method and its characterization*, **Thin Solid Films**, **515**, **(4)**, pp. 1912–1917, Dec. 2006, doi: 10.1016/j.tsf.2006.07.035.

[23] A. L. Rogach, *Nanocrystalline CdTe and CdTe(S) particles: wet chemical preparation, size-dependent optical properties and perspectives of optoelectronic applications*, **Mater. Sci.**

Eng. B, **69–70**, pp. 435–440, Jan. 2000, doi: 10.1016/S0921-5107(99)00231-7.

[24] O. Toma *et al.*, *Physical properties of rf-sputtered ZnS and ZnSe thin films used for double-heterojunction ZnS/ZnSe/CdTe photovoltaic structures*, **Appl. Surf. Sci.**, **478**, pp. 831–839, Jun. 2019, doi: 10.1016/j.apsusc.2019.02.032.

[25] J. Vidal, O. de Melo, O. Vigil, N. López, G. Contreras-Puente, and O. Zelaya-Angel, *Influence of magnetic field and type of substrate on the growth of ZnS films by chemical bath*, **Thin Solid Films**, **419**, **(1–2)**, pp. 118–123, Nov. 2002, doi: 10.1016/S0040-6090(02)00767-8.

[26] T. A. Safeera, N. Johns, and E. I. Anila, *Effect of anionic concentration on the structural and optical properties of nanostructured ZnS thin films*, **Opt. Mater. (Amst).**, **58**, pp. **32–37**, Aug. 2016, doi: 10.1016/j.optmat.2016.03.050.

[27] S. Tec-Yam, J. Rojas, V. Rejón, and A. I. Oliva, *High quality antireflective ZnS thin films prepared by chemical bath deposition*, **Mater. Chem. Phys.**, **136**, **(2–3)**, pp. 386–393, Oct. 2012, doi: 10.1016/j.matchemphys.2012.06.063.

[28] D. Moore and Z. L. Wang, *Growth of anisotropic one-dimensional ZnS nanostructures*, **J. Mater. Chem.**, **16**, **(40)**, p. 3898, 2006, doi: 10.1039/b607902b.

[29] Y. Yusoff, P. Chelvanathan, N. Kamaruddin, M. Akhtaruzzaman, and N. Amin, *A low cost and single source atmospheric pressure vapor phase epitaxy of ZnS for thin film photovoltaic applications*, **Mater. Lett.**, **221**, pp. 216–219, Jun. 2018, doi: 10.1016/j.matlet.2018.03.096.

[30] R. Vishwakarma, *Effect of substrate temperature on ZnS films prepared by thermal evaporation technique*, **J. Theor. Appl. Phys.**, **9**, **(3)**, pp. 185–192, Sep. 2015, doi: 10.1007/s40094-015-0177-5.

[31] P. K. Nair and M. T. S. Nair, *Chemically deposited ZnS thin films: application as substrate for chemically deposited* Bi_2S_3, Cu_xS *and PbS thin films*, **Semicond. Sci. Technol.**, **7**, **(2)**, pp. 239–244, Feb. 1992, doi: 10.1088/0268-1242/7/2/011.

[32] M. Yoneta, M. Ohishi, H. Saito, and T. Hamasaki, *Low temperature molecular beam epitaxial growth of ZnS/GaAs(001) by using elemental sulfur source*, **J. Cryst. Growth**, **127**, **(1–4)**, pp. 314–317, Feb. 1993, doi: 10.1016/0022-0248(93)90628-A.

[33] A. Abounadi *et al.*, *Reflectivity and photoluminescence measurements in ZnS epilayers grown by metal-organic chemical-vapor deposition*, **Phys. Rev. B**, **50**, **(16)**, pp. 11677–11683, Oct. 1994, doi: 10.1103/PhysRevB.50.11677.

[34] N. Poornima, A. Jose, C. S. Kartha, and K. P. Vijayakumar, *Composition and Conductivity-type Analysis of Spray Pyrolysed ZnS Thin Films using Photoluminescence*, **Energy Procedia**, **15**, pp. 347–353, 2012, doi: 10.1016/j.egypro.2012.02.042.

[35] M. S. Akhtar, S. Riaz, and S. Naseem, *Optical Properties of Sol-gel Deposited ZnS Thin Films: Spectroscopic Ellipsometry*, **Mater. Today Proc.**, **2**, **(10)**, pp. 5497–5503, 2015, doi: 10.1016/j.matpr.2015.11.076.

[36] D. Saikia, P. K. Saikia, P. K. Gogoi, M. R. Das, P. Sengupta, and M. V. Shelke, *Synthesis and characterization of CdS/PVA nanocomposite thin films from a complexing agent free system*, **Mater. Chem. Phys.**, **131**, **(1–2)**, pp. 223–229, Dec. 2011, doi: 10.1016/j.matchemphys.2011.09.011.

[37] G. L. Agawane *et al.*, *Non-toxic complexing agent Tri-sodium citrate's effect on chemical bath deposited ZnS thin films and its growth mechanism*, **J. Alloys Compd.**, **535**, pp. 53–61, Sep. 2012, doi: 10.1016/j.jallcom.2012.04.073.

[38] J. Zhu, M. Zhou, J. Xu, and X. Liao, *Preparation of CdS and ZnS nanoparticles using microwave irradiation*, **Mater. Lett.**, **47**, **(1–2)**, pp. 25–29, Jan. 2001, doi: 10.1016/S0167-577X(00)00206-8.

[39] Q. Zhao, L. Hou, and R. Huang, *Synthesis of ZnS nanorods by a surfactant-assisted soft chemistry method*, **Inorg. Chem. Commun.**, **6**, **(7)**, pp. 971–973, Jul. 2003, doi: 10.1016/S1387-7003(03)00146-1.

[40] R. R. Salunkhe, D. S. Dhawale, T. P. Gujar, and C. D. Lokhande, *Structural, electrical and optical studies of SILAR deposited cadmium oxide thin films: Annealing effect*, **Mater. Res. Bull.**, **44**, **(2)**, pp. 364–368, Feb. 2009, doi: 10.1016/j.materresbull.2008.05.010.

[41] D. Beckel *et al.*, *Thin films for micro solid oxide fuel cells*, **J. Power Sources**, **173**, **(1)**, pp. 325–345, Nov. 2007, doi: 10.1016/j.jpowsour.2007.04.070.

[42] G. Binnig, C. F. Quate, and C. Gerber, *Atomic Force Microscope*, **Phys. Rev. Lett.**, **56**, **(9)**, pp. 930–933, Mar. 1986, doi: 10.1103/PhysRevLett.56.930.

[43] M. Zuo, S. Tan, G. Li, and S. Zhang, *Structure characterization, magnetic and photoluminescence properties of Mn doped ZnS nanocrystalline*, **Sci. China Physics, Mech. Astron.**, **55**, **(2)**, pp. 219–223, Feb. 2012, doi: 10.1007/s11433-011-4595-3.

[44] P. Dhingra, P. Singh, P. J. S. Rana, A. Garg, and P. Kar, *Hole-Transporting Materials for Perovskite-Sensitized Solar Cells*, **Energy Technol.**, **4**, **(8)**, pp. 891–938, Aug. 2016, doi: 10.1002/ente.201500534.

[45] J. Tauc, *Optical properties and electronic structure of amorphous Ge and Si*, **Mater. Res. Bull.**, **3**, **(1)**, pp. 37–46, Jan. 1968, doi: 10.1016/0025-5408(68)90023-8.

[46] J. Santos *et al.*, *Hole-Transporting Materials for Perovskite Solar Cells Employing an Anthradithiophene Core*, **ACS Appl. Mater. Interfaces**, **13**, **(24)**, pp. 28214–28221, Jun. 2021, doi: 10.1021/acsami.1c05890.

[47] N. ÜZAR and M. Ç. ARIKAN, *Synthesis and investigation of optical properties of ZnS nanostructures*, **Bull. Mater. Sci.**, **34**, **(2)**, pp. 287–292, Apr. 2011, doi: 10.1007/s12034-011-0085-5.

[48] A. L. Patterson, *The Scherrer Formula for X-Ray Particle Size Determination*, **Phys. Rev.**, **56**, **(10)**, pp. 978–982, Nov. 1939, doi: 10.1103/PhysRev.56.978.

Received: September 21, 2023
Accepted: October 19, 2023